Simultaneous Cyclic Scheduling and Control of a Multiproduct CSTR

Antonio Flores-Tlacuahuac*

Departamento de Ingeniería y Ciencias Químicas, Universidad Iberoamericana, Prolongación Paseo de la Reforma 880, México D.F. 01210, México

Ignacio E. Grossmann

Department of Chemical Engineering, Carnegie-Mellon University, 5000 Forbes Avenue, Pittsburgh, Pennsylvania 15213

In this work, we propose a simultaneous scheduling and control formulation by explicitly incorporating into the scheduling model process dynamics in the form of differential/algebraic constraints. The formulation takes into account the interactions between scheduling and control and is able to handle nonlinearities embedded into the processing system. The simultaneous scheduling and control problems is cast as a mixed-integer dynamic optimization (MIDO) problem where the simultaneous approach, based on orthogonal collocation on finite elements, is used to transform it into a mixed-integer nonlinear programming (MINLP) problem. The proposed simultaneous scheduling and control formulation is tested using three multiproduct continuous stirred tank reactors featuring difficult nonlinearities.

1. Introduction

Traditionally, scheduling and control (SC) problems in chemical processes have been addressed separately. From a scheduling point of view, the interest lies in determining optimal assignments to equipment production sequences, production times for each product, and inventory levels that lead to maximum profit or minimum completion time.[1] Commonly, during this task, the dynamic behavior of the underlying process is not taken into account. Similarly, when computing optimal transition trajectories (i.e., optimal values of the manipulated and controlled variables) between different set of products, one of the major objectives lies in determining the transition trajectory featuring minimum transition time.[2] When addressing optimal control problems, it is normally assumed that the production sequence is fixed.[3] Hence, scheduling decisions are normally neglected in optimal control formulations. In pure scheduling problems, the transition times between the different product combinations are assumed to be known as fixed values, and hence, the dynamic profile of the chosen manipulated and controlled variables is not taken into account in the optimization formulation.

It has been recognized,[4−7] however, that scheduling and control problems are closely related problems and that, ideally, they should be addressed simultaneously rather than sequentially or solved without taking into account both parts. In this work, the interactions between scheduling and control problems are taken into account with the proposed formulation, therefore leading to improvements in the objective function value and avoiding suboptimal solutions.

Some early attempts to address the scheduling and dynamic optimization problem were made by Bhatia and Biegler,[4] who used the aggregate scheduling model by Birewar and Grossmann[8] to optimize the sizing, scheduling, and processing times using a nonlinear programming (NLP) model. Mahadevan et al.[5] analyzed grade transition scheduling problems from a robust closed-loop point of view. These authors did not address the

problem as a mixed-integer dynamic optimization (MIDO) problem, although it is recognized that optimal grade transition and scheduling problems should be approached along this line. They obtained grade schedules by defining easy and hard to carry out transitions. Chatzidoukas et al.[9] proposed a MIDO formulation for analyzing polymer grade transition and optimal campaign scheduling. For solving the MIDO problem, they used the algorithm proposed by Allgor and Barton.[10] Smania and Pinto[11] used steady-state models, and discrete time decisions, for optimizing production campaigns.

There have been more recents papers addressing the scheduling and control problem. Mishra et al.[6] made a comparison between what they denote as the standard recipe approach (SRA) and the overall optimization approach (OOA) for solving SC problems. In the SRA approach, process dynamics, through the direct incorporation of a process mathematical model, is neglected, and in its place a set of correlations, obtained from running local optimizations, are developed to capture time domain behavior. On the other hand, in the OOA approach, the process dynamic model is included into the formulation. The set of ordinary differential equations modeling the related process are discretized and transformed into a set of algebraic equations.[12−14] In particular in ref 14, the authors added dynamics to state task networks (STN), creating a very large and difficult to solve problem. In the present work, we are only adding dynamics to a single unit/single stage. We think that, even when at first sight the approach used in ref 14 and our MIDO strategy might look similar, they are not. Our MIDO formulation is significantly smaller than that in ref 14, therefore leading to a mixed-integer nonlinear programming (MINLP) problem that is easier to solve. Hence, in the OOA method, the resulting SC problem is cast as an MINLP problem. In ref 6, the authors claim that, because in the OOA method the number of available degrees of freedom is larger than in the SRA method, the optimal solution obtained by using the OOA method will be superior to the one obtained using the SRA method, as their two cases of study show. Although the superiority of the OOA method for addressing SC problems is clear from their examples, they concluded that the use of the discretization approach to transform a MIDO problem into an MINLP problem

---

* To whom correspondence should be addressed. E-mail: antonio.flores@uia.mx. Phone/Fax: +52(55)59594074. http://200.13.98.241/~antonio.

is not feasible because of the large of number of constraints generated when discretizing the process dynamic model. Moreover, the authors solved the MINLP problems by a direct approach, meaning that they did not use any decomposition solution strategy aimed to reduce the computational complexity faced when solving MIDO problems. They concluded that additional work is needed to improve MIDO solution techniques. There have been some other approaches using sequential methods for MIDO problem solutions.[15,16] In this approach, only the controlled variables are discretized; the values of the time-dependent optimal manipulated variables are computed trough numerical integration. There have been some recent research efforts[17] trying to guarantee global optimality when solving MIDO problems by sequential methods.

In another recent work,[17] scheduling and grade transition for polymerization systems has been addressed. The authors proposed a decomposition scheme specifically tailored for the resulting MIDO problem. On the basis of previous work on MIDO problem solution strategies,[10] the authors proposed to solve the MIDO problem as a sequence of primal and master problems. The primal problem contains the dynamic optimization part, while the master problem deals with the scheduling part. The authors report good convergence properties when analyzing scheduling and grade transition for a polymerization plant; however, no details of the specific polymerization system are given. As the authors recognize, their MIDO solution strategy is highly application specific, and therefore, it would be difficult to apply to other polymerization systems. Without enough details about the polymerization process dynamics and nonlinearities embedded, it is difficult to assess the robustness of the solution strategy.

In this work, we propose a simultaneous approach to address scheduling and control problems for a continuous stirred tank reactor (CSTR) that produces multiple products. We take advantage of the rich knowledge of scheduling and optimal control formulations, and we merge them so the final result is a formulation able to solve simultaneous scheduling and control problems. We cast the problem as an optimization problem. In the proposed formulation, integer variables are used to determine the best production sequence and continuous variables take into account production times, cycle time, and inventories. Because dynamic profiles of both manipulated and controlled variables are also decision variables, the resulting problem is cast as a mixed-integer dynamic optimization (MIDO) problem. To solve the MIDO problem, we use a recently proposed methodology[18] that consists of transforming the MIDO problem into an MINLP that can be solved using standard methods such as the outer-approximation method.[19,20] Roughly speaking, the strategy for solving the MIDO problem consists of using the so-called simultaneous approach[2] for solving optimal control problems as the way to transform the set of ordinary differential equations modeling the dynamic system behavior into a set of algebraic equations. Because of the highly nonlinear behavior embedded in chemical process models, the resulting MIDO formulation will be an MINLP problem featuring difficult nonlinearities such as multiple steady states, parametric sensitivity, bifurcation, and even chaotic dynamics. In summary, the contributions made in this work are as follows: (a) a complete and more general scheduling formulation is used; (b) a robust and numerically stable simultaneous method is used for approaching the dynamic optimization phase; and (c) the relationship between nonlinear behavior and complexity for solving the MIDO problem has been addressed.
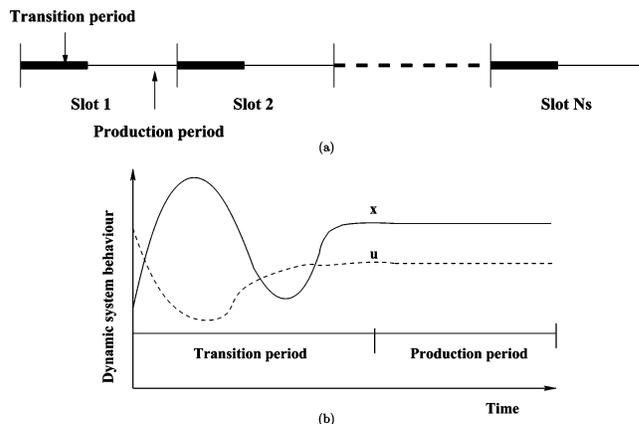
Figure 1. (a) The cyclic time is divided into slots, and within each slot, a steady-state production period is followed by a transition period. (b) Within each slot, the system states x and the manipulated variables u remain constant. However, during the transition period, the manipulated variables change and so do the system states.

2. Problem Definition

Given are a number of products that are to be manufactured in a single continuous multiproduct CSTR. Lower bounds for the product demands expressed as constant rates are specified. Steady-state operating conditions for manufacturing each product are also specified, as well as the price of each product and the inventory and raw materials costs. The problem then consists of the simultaneous determination of a cyclic schedule (i.e., production wheel) and the control profile for the selected transitions. The major decisions involve selecting the sequence (i.e., cyclic time and the sequence in which the products will be manufactured) as well as the transition times, production rates, length of processing times, amounts manufactured of each product, and manipulated variables for the transition such that the profit is maximized.

We should note that the reason the proposed scheduling problem involves a production wheel with a cyclic schedule is because the demand rates are assumed to be a constant. Therefore, the key tradeoffs in determining the cycle time and the sequence in this problem are between inventory and transition costs as discussed by Pinto and Grossmann.[21] Also note that a cyclic schedule is equivalent to considering an infinite horizon in which the cyclic schedule is repeated an infinite number of times. Such a schedule is only valid and relevant when the demand rates are constant or nearly constant, as assumed in this paper.

3. Scheduling and Control MIDO Formulation

In the following simultaneous scheduling and control (SSC) formulation, we assume that all products are manufactured in a single CSTR and that the products follow a production wheel, meaning that all the required products are manufactured, in an optimal cyclic sequence (see ref 21 for the scheduling formulation). As shown in Figure 1a, the cycle time is divided into a series of time slots. Within each slot, two operations are carried out: (a) the transition period, during which dynamic transitions between two products take place, and (b) the production period, during which a given product is manufactured around steady-state conditions. According to this description, Figure 1b depicts a typical dynamic operating response curve within each slot. At the beginning of each slot, the CSTR process conditions are changed (by modifying the manipulated variables u) until new desired process operating conditions (as represented by the system states x), leading to the manufacture of a new product,

are reached. Afterward, material of the new given product is manufactured until the demand imposed on such product is met; during this period, both the system states x and the manipulated variables u remain constant. In this work, we assume that each product is produced only once within each production wheel. Also, we assume that, once a production wheel is completed, new identical cycles are executed indefinitely. Notice that one slot equals one transition.

To clarify the simultaneous SC MIDO problem formulation, it has been divided into two parts. The first one deals with the scheduling part, and the second one deals with the dynamic optimization part.

3.1. Objective Function.

$$\max\{\phi_1 + \phi_2 - \phi_3\} \tag{1}$$

where ϕ_1 deals with the product profits, ϕ_2 deals with the inventory costs, and ϕ_3 deals with the transition costs; these are defined as follows,

$$\phi_1 = \sum_{i=1}^{N_p} \frac{C_i^p W_i}{T_c} \tag{2}$$

$$\phi_2 = \sum_{i=1}^{N_p} \frac{C_i^s(G_i - W_i/T_c)}{2\Theta_i} \tag{3}$$

$$\phi_3 = \sum_{k=1}^{N_s} \sum_{f=1}^{N_{fe}} h_{fk} \sum_{c=1}^{N_{cp}} \frac{C^r t_{fck} \Omega_{c,N_{cp}}}{T_c} ((x^1_{fck} - \bar{x}^1_k)^2 + ... + (x^n_{fck} - \bar{x}^n_k)^2 + (u^1_{fck} - \bar{u}^1_k)^2 + ... + (u^m_{fck} - \bar{u}^m_k)^2) \tag{4}$$

As shown, the total process profit is given by the amount and cost of the manufactured products minus the sum of the inventory costs and the product transition costs. As a measure of the transition costs, we use a term that takes into account the amount of off-specification material produced during product transition. At each slot, such a term has the following form,

$$\frac{1}{T_c} \int_0^{t_f} [\sum_n (x^n - \bar{x}^n)^2 + \sum_m (u^m - \bar{u}^m)^2]C^r \, dt \tag{5}$$

where t_f is the transition time in slot k, C^r is the cost of the raw material, T_c is the duration of the production wheel cycle, x^n is the nth system state, and $\bar{x}^n$ is its desired value. Similarly, u^m is the mth manipulated variable and $\bar{u}^m$ is its desired value. The above integral can be approximated by Radau quadrature as follows:

$$\sum_{k=1}^{N_s} \sum_{f=1}^{N_{fe}} h_{fk} \sum_{c=1}^{N_{pc}} \frac{C^r t_{fck} \Omega_{c,N_{cp}}}{T_c} ((x^1_{fck} - \bar{x}^1_k)^2 + ... + (x^n_{fck} - \bar{x}^n_k)^2 + (u^1_{fck} - \bar{u}^1_k)^2 + ... + (u^m_{fck} - \bar{u}^m_k)^2)$$

It should be noted that this form of the transition costs will force the system to carry out product transitions as soon as possible, while at the end of a product transition, the states will take the steady-state values for manufacturing a new product.

Sometimes products' quality are specified by lower and upper limits around a central nominal value. Imposing upper and lower limits in the specification of products would simply require the replacement of endpoint equations by endpoint inequality constraints in the dynamic optimization problem discussed later.

Similarly, a more general objective function could be added to minimize out-of-spec material or maximize productivity. One could then certainly apply the proposed simultaneous scheduling and control strategy to an extended version of this problem.

3.1.1. Scheduling Part. 3.1.1.a. Product Assignment.

$$\sum_{k=1}^{N_s} y_{ik} = 1, \forall i \tag{6a}$$

$$\sum_{i=1}^{N_p} y_{ik} = 1, \forall k \tag{6b}$$

$$y'_{ik} = y_{i,k-1}, \forall i, k \neq 1 \tag{6c}$$

$$y'_{i,1} = y_{i,N_s}, \forall i \tag{6d}$$

Equation 6a states that, within each production wheel, any product can only be manufactured once, while constraint 6b implies that only one product is manufactured at each time slot. Because of this constraint, the number of products and slots turns out to be the same. Equation 6c defines a backward binary variable (y'_{ik}), meaning that such a variable for product i in slot k takes the value assigned to the same binary variable but one slot backward, $k - 1$. At the first slot, eq 6d defines the backward binary variable as the value of the same variable at the last slot. This type of assignment reflects our assumption of cyclic production wheel. The variable y'_{ik} will be used later to determine the sequence of product transitions.

3.1.1.b. Amounts Manufactured.

$$W_i \geq D_i T_c, \forall i \tag{7a}$$

$$W_i = G_i \Theta_i, \forall i \tag{7b}$$

$$G_i = F^\circ(1 - X_i), \forall i \tag{7c}$$

Equation 7a states that the total amount manufactured of each product i must be equal to or greater than the desired demand rate times the duration of the production wheel, while eq 7b indicates that the amount manufactured of product i is computed as the product of the production rate (G_i) times the time used (Θ_i) for manufacturing such product. The production rate is computed from eq 7c as a simple relationship between the feed stream flow rate (F°) and the conversion (X_i).

3.1.1.c. Processing Times.
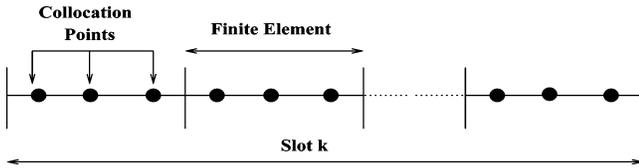
$$\theta_{ik} \leq q^{max} y_{ik}, \forall i, k \tag{8a}$$

$$\Theta_i = \sum_{k=1}^{N_a} \theta_{ik}, \forall i \tag{8b}$$

$$p_k = \sum_{i=1}^{N_p} \theta_{ik}, \forall k \tag{8c}$$

The constraint given by eq 8a sets an upper bound on the time used for manufacturing product i at slot k. Equation 8b is the time used for manufacturing product i, while eq 8c defines the duration time at slot k.

3.1.1.d. Transitions between Products.

$$z_{ipk} \geq y'_{pk} + y_{ik} - 1, \forall i, p, k \tag{9}$$

Figure 2. Simultaneous discretization approach for dealing with dynamic optimization problems. Each slot k is divided into N_{fe} finite elements. Within each finite element f, a set of N_{cp} collocation points c is selected.

The constraint given in eq 9 is used for defining the binary production transition variable z_{ipk}. If such variable is equal to 1, then a dynamic transition will occur from product i to product p within slot k; z_{ipk} will be zero otherwise.

3.1.1.e. Timing Relations.

$$\theta_k^{\text{t}} = \sum_{i=1}^{N_{\text{p}}} \sum_{p=1}^{N_{\text{p}}} t_{pi}^{\text{t}} z_{ipk}, \ \forall k \tag{10a}$$

$$t_1^{\text{s}} = 0 \tag{10b}$$

$$t_k^{\text{e}} = t_k^{\text{s}} + p_k + \sum_{i=1}^{N_{\text{p}}} \sum_{p=1}^{N_{\text{p}}} t_{pi}^{\text{t}} z_{ipk}, \ \forall k \tag{10c}$$

$$t_k^{\text{s}} = t_{k-1}^{\text{e}}, \ \forall k \neq 1 \tag{10d}$$

$$t_k^{\text{e}} \leq T_{\text{c}}, \ \forall k \tag{10e}$$

$$t_{fck} = (f-1)\frac{\theta_k^{\text{t}}}{N_{\text{fe}}} + \frac{\theta_k^{\text{t}}}{N_{\text{fe}}} \gamma_{\text{c}}, \ \forall f, c, k \tag{10f}$$

Equation 10a defines the transition time from product i to product p at slot k. It should be remarked that the term t_{pi}^{t} stands only for an estimate of the expected transition times. Because such transition times depend on process dynamic behavior, they will be computed iteratively as part of the scheduling and control formulation. Good initial estimates of the transition times can be obtained from open-loop dynamic optimization runs between all pairs of products. If the transition times happen to be difficult to evaluate, or if the number of combinations of product schedules turns out to be large, t_{pi}^{t} values could be set as $4\times$ the reactor open-loop residence time. First, one needs to guess transition time values (t_{pi}^{t}), solve the MIDO problem, and check if the computed transition time values (θ_k^{t}) are long enough to allow safe and smooth grade transition dynamic behavior. Frequently, large dynamic variations in the states and manipulated variables behavior are an indication that, by increasing the guessed t_{pi}^{t} values, better and smoother dynamic grade transition behavior could be obtained. Normally, in few iterations, one can easily obtain acceptable grade transition dynamic behavior. Equation 10b sets to zero the time at the beginning of the production wheel cycle corresponding to the first slot. Equation 10c is used for computing the time at the end of each slot as the sum of the slot start time plus the processing time and the transition time. Equation 10d states that the start time at all the slots, different than the first one, is just the end time of the previous slot. Equation 10e is used to force that the end time at each slot be less than the production wheel cyclic time. Finally, eq 10f is used to obtain the time value inside each finite element and for each internal collocation point.

3.1.2. Dynamic Optimization Part. To address the optimal control part, the simultaneous approach[2] for solving dynamic optimization problems was used. In this approach, the dynamic model representing the system behavior is discretized using the method of orthogonal collocation on finite elements.[22,23] According to this procedure, a given slot k is divided into a number of finite elements. Within each finite element, an adequate number of internal collocation points is selected, as depicted in Figure 2. Using several finite elements is useful to represent dynamic profiles with nonsmooth variations. Thereby, the set of ordinary differential equations comprising the system model is approximated at each collocation point, leading to a set of nonlinear equations that must be satisfied.

3.1.2.a. Dynamic Mathematical Model Discretization.

$$x_{fck}^n = x_{\text{o},fk}^n + \theta_k^{\text{t}} h_{fk} \sum_{l=1}^{N_{\text{cp}}} \Omega_{lc}\, \dot{x}_{flk}^n, \ \forall n, f, c, k \tag{11}$$

The constraints given by eq 11 are used to compute the value of the system states at each one of the discretized points (x_{fck}^n) by using the monomial basis representation. $x_{\text{o},fk}^n$ is the nth system state at the beginning of each element, Ω_{lc} is the collocation matrix, and $\dot{x}_{fck}^n$ is the first-order derivative of the nth state. Notice that, when working with the first element, $x_{\text{o},1k}^n$ represents the specified initial value of the nth state. Also notice that, in the present formulation, the length of all finite elements is the same and computed as

$$h_{fk} = \frac{1}{N_{\text{fe}}} \tag{12}$$

3.1.2.b. Continuity Constraint between Finite Elements.

$$x_{\text{o},fk}^n = x_{\text{o},f-1,k}^n + \theta_k^{\text{t}} h_{f-1,k} \sum_{l=1}^{N_{\text{cp}}} \Omega_{l,N_{\text{cp}}}\, \dot{x}_{f-1,l,k}^n, \ \forall n, f \geq 2, k \tag{13}$$

In the simultaneous approach for dynamic optimization problems, only the states must be continuous when crossing from one given finite element to the next one; algebraic and manipulated variables are allowed to exhibit discontinuity behavior between adjacent finite elements. That is the reason continuity constraints are not formulated for algebraic and manipulated variables. We use eq 13 to force continuous state profiles on all the elements at the beginning of each element ($x_{\text{o},fk}^n$), and they are computed in terms of the same monomial basis used before for defining the value of the system states.

3.1.2.c. Model Behavior at Each Collocation Point.

$$\dot{x}_{fck}^n = f^n(x_{fck}^1, ..., x_{fck}^n, u_{fck}^1, ..., u_{fck}^m), \ \forall n, f, c, k \tag{14}$$

Equation 14 is used for computing the value of the first-order derivatives of the systems at finite element f of collocation point c in slot k. Those equations simply represet the right-hand sides of the dynamic model. Because our scheduling and control formulation is system independent, we have used the notation f^n to represent the right-hand side of the nth ordinary differential equation describing any desired dynamic system.

3.1.2.d. Initial and Final Controlled and Manipulated Variable Values at Each Slot.

$$x_{\text{in},1}^n = \sum_{i=1}^{N_{\text{p}}} x_{\text{ss},i}^n y_{i,N_s}, \ \forall n \tag{15}$$

$$x_{\text{in},k}^n = \sum_{i=1}^{N_{\text{p}}} x_{\text{ss},i}^n y_{i,k-1}, \ \forall n, k \neq 1 \tag{16}$$

$$\tilde{x}_k^n = \sum_{i=1}^{N_p} x_{ss,i}^n y_{i,k}, \forall n, k \tag{17}$$

$$u_{in,1}^m = \sum_{i=1}^{N_p} u_{ss,i}^m y_{i,N_s}, \forall m \tag{18}$$

$$u_{in,k}^m = \sum_{i=1}^{N_p} u_{ss,i}^m y_{i,k-1}, \forall m, k \neq 1 \tag{19}$$

$$\bar{u}_k^m = \sum_{i=1}^{N_p} u_{ss,i}^m y_{i,k}, \forall m, k \tag{20}$$

$$u_{1,1,k}^m = u_{in,k}^m, \forall m, k \tag{21}$$

$$u_{N_{fe},N_{cp},k}^m = \bar{u}_{in,k}^m, \forall m, k \tag{22}$$

$$x_{o,1,k}^n = x_{in,k}^n, \forall n, k \tag{23}$$

The desired value of each state at the beginning of slot k ($x_{in,k}^n$) is computed in eqs 15 and 16. Equation 17 define the values of the state variables at the end of each slot k ($\bar{x}_k^n$). It should be stressed that the state values at the beginning and end of each slot k are given by the corresponding steady-state values ($x_{ss,i}^n$) calculated a priori. $x_{ss,i}^n$ simply stands for the steady-state value of the manufacturing product i. They can be easily obtained from open-loop steady-state simulation of the processing system. Similarly, eqs 18 and 19 define the values of the manipulated variables at the beginning of each slot k ($u_{in,k}^m$) and at the end of the slot k ($\bar{u}_k^m$). Equation 20 enforces the system states to take the desired state values at each slot k. A similar situation occurs with the values of the manipulated variables. Equation 21 fixes the values at the first finite element and first collocation point of each slot k ($u_{1,1,k}^m$) as the value that such variable takes at the beginning of the same slot k. Equation 22 determines the values of the manipulated variables at the last finite element and last collocation point of slot k ($u_{N_{fe},N_{cp},k}^m$) as the desired steady-state value of the same variable at slot k ($\bar{u}_k^m$). Finally, eq 23 determines the values of the system states at the beginning of each slot ($x_{o,1,k}^n$).

3.1.2.e. Lower and Upper Bounds on the Decision Variables.

$$x_{min}^n \leq x_{fck}^n \leq x_{max}^n, \forall n, f, c, k \tag{24a}$$

$$u_{min}^m \leq u_{fck}^m \leq u_{max}^m, \forall m, f, c, k \tag{24b}$$

Equations 24a and 24b simply constrain the values of both the system states and manipulated variables to lie within acceptable lower and upper bounds.

3.2. Solution Algorithm. To solve the simultaneous scheduling and control problem, the simultaneous approach for solving dynamic optimization problems was used to transform the MIDO problem into an MINLP whose solution was attempted by the well-known outer approximation approach[20] as implemented in the DICOPT software. Although the solution of the resulting MINLP is direct, the determination of some variables related to the dynamic optimization part requires an iterative procedure. The transition times t_{pi}^t and the number of finite elements N_{fe} are the two main variables that must be determined in an iterative manner. Initially t_{pi}^t can be set to an upper value
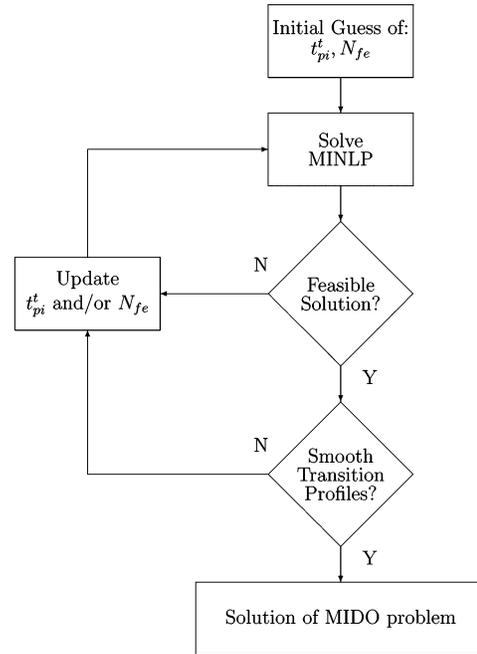
Figure 3. Iterative algorithm for the solution of the simultaneous scheduling and control problem.

of 4× the reactor open-loop residence time, while setting N_{fe} = 20 tends to produce good dynamic transition profiles. Of course, both variables need to be updated depending upon the quality of the results and/or if the MINLP turns out to be infeasible for a set of t_{pi}^t and N_{fe} guessed values. Figure 3 depicts the iterative procedure that was used to solve the simultaneous scheduling and control problem. Since we rely on local NLP solvers, and no special provisions are taken to rigorously estimate the bounds with the MILP master problem, the global optimum solution cannot be guaranteed. As will be seen in the examples, useful solutions can still be obtained with the proposed approach.

It should be stressed that, although the transition times t_{pi}^t are not considered as decision variables, the transition times obtained from the algorithm depicted in Figure 3 will be very close to those obtained by considering t_{pi}^t as decision variables. The only reason to prefer the optimization formulation as presented in this work, compared to the case in which the transition time becomes a decision variable, is because the present optimization formulation is simpler to deal with. Insisting in using the transition time as a decision variable will only increase the nonconvexity of the underlying optimization formulation. Therefore, according to our experience, solving scheduling and control MIDO problems, as proposed in the present paper, will make it easier to solve the resulting optimization problem

4. Case Studies

To test the proposed simultaneous scheduling and control formulation, three case studies, with different numbers of products and different degrees of nonlinear behavior embedded in the model, were addressed. In all the cases, CSTRs were used to manufacture the desired products. The case studies range from CSTRs featuring quasi-linear behavior (first case study) to CSTRs with input multiplicities (second case study) and output multiplicities (third case study). In all the cases with embedded nonlinear behavior, the operating conditions were chosen around nonlinear behavior regions. We did so because

Table 1. Process Data for the First Case Study[a]

product	Q (L/h)	C_R (mol/L)	demand rate (kg/h)	product cost ($/kg)	inventory cost ($)
A	10	0.0967	3	200	1
B	100	0.2	8	150	1.5
C	400	0.3032	10	130	1.8
D	1000	0.393	10	125	2
E	2500	0.5	10	120	1.7

[a] A, B, C, D, and E stand for the five products to be manufactured. The cost of the Raw Material (C^r) Is $10.

Table 2. Simultaneous Scheduling and Control Results for the First Case Study[a]

slot	product	process time (h)	production rate (kg/h)	w (kg)	transition time (h)	T start (h)	T end (h)
1	A	41.5	9.033	374.31	5	0	46.4
2	E	23.3	1250	29 162.3	5	46.4	74.7
3	D	2.06	607	1 247.7	5	74.7	81.8
4	C	4.48	278.72	1 247.7	5	81.8	91.2
5	B	12.48	80	998.2	21	91.2	124.7

[a] The objective function value is $7889 and 124.8 h of total cycle time.

Table 3. Simultaneous Scheduling and Control Results for the First Case Study, Second Best Solution[a]

slot	product	process time (h)	production rate (kg/h)	w (kg)	transition time (h)	T start (h)	T end (h)
1	A	41.5	9.033	374.31	5	0	46.4
2	D	2.06	607	1 249.4	5	46.4	53.6
3	E	23.4	1250	29 270.4	5	53.6	82
4	C	4.48	278.72	1 249.4	5	82	91.5
5	B	12.48	80	999.5	21	91.5	125

[a] The objective function value is $7791 and 125 h of total cycle time.

most chemical processes featuring optimality conditions tend to exhibit regions of highly nonlinear behavior[24] and to have an exact idea about the complexities of solving MIDO problems with embedded nonlinearities. Hopefully, this will allow us to identify research areas where MIDO formulations/algorithms require improvements.

4.1. CSTR with a Simple Irreversible Reaction. The following reaction,

$$3R \xrightarrow{k} P, \quad -\mathscr{R}_R = kC_R{}^3$$

takes place in an isothermal CSTR for manufacturing five products, A, B, C, D, and E. The dynamic composition model is given by

$$\frac{dC_R}{dt} = \frac{Q}{V}(C_o - C_R) + \mathscr{R}_R \quad (25)$$

where C_o stands for feed stream composition and Q is the control variable for the dynamic transition in the production of one product to another. Using the following values of the design and kinetic parameters, $C_o = 1$ mol/L, $V = 5000$ L, $k = 2$ L^2/(mol^2·h), and the five values of the volumetric flowrate Q shown in Table 1, the five concentration steady states C_R, shown in the same table, are obtained. All the examples featured in this work require the steady-states values of the manipulated (u) and controlled variables (x) for manufacturing each one of the products. In addition, Table 1 also features values of the demand rate (D_i), product cost (C_i^p), and inventory cost (C_i^s).

Solving the MIDO scheduling and control problem using GAMS/DICOPT, the optimizer selects the cyclic A → E → D
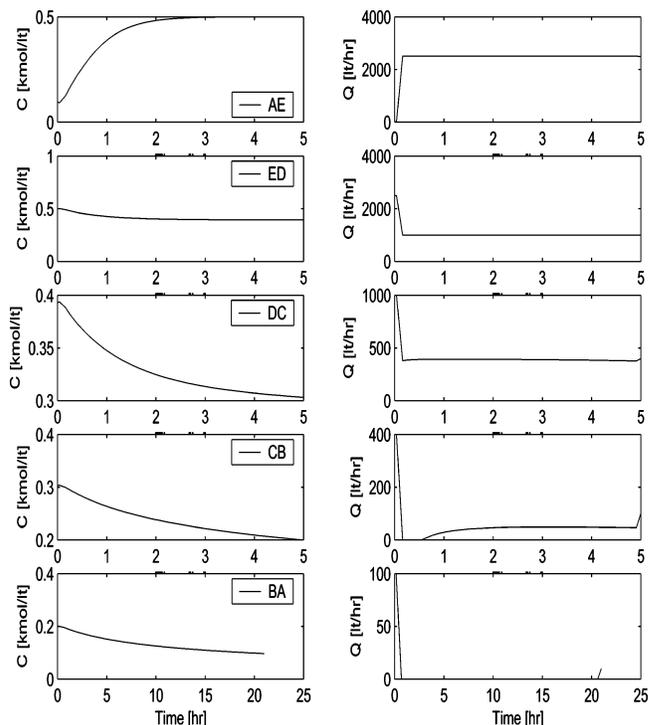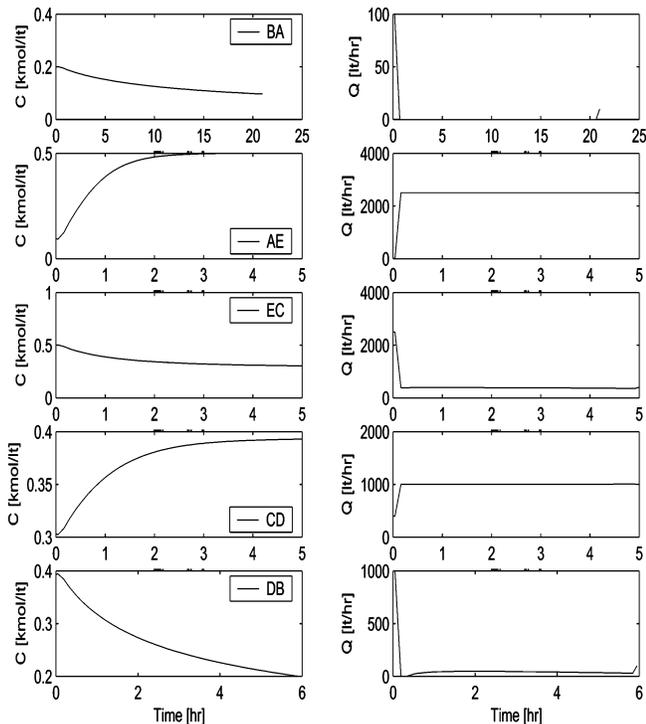

Figure 4. Optimal dynamic profiles for the volumetric flow rate and reactor concentration during product transition for the first case study.

→ C → B production wheel as the one which maximizes the profit. The objective function value turned out to be $7889, while the total cycle time was 124.8 h. Additional information concerning processing times at each slot, production rates, total amounts of each product, transition times, and initial and ending times at each slot are shown in Table 2. Regarding the dynamic behavior of the reactor during product transitions, Figure 4 displays the dynamic profiles of both the manipulated variable (Q) and the controlled variable (C_R). It is interesting to note that, if the transition times were to be reduced by 1 h, the optimal sequence changes to E → D → C → B → A and the objective function increases to $9685, which shows the impact of optimizing the transition times in this problem.

It is interesting to compare the optimal MIDO solution against the second- and third-best cyclic solutions. Moreover, to compare the performance of DICOPT when solving MIDO problems, the second- and third-best optimal solutions of all the examples were always computed using SBB (other MINLP solver available in GAMS). In the present example, the second best solution, which was obtained by adding an integer cut, is in fact a slight variation of the previous one. In this case, the optimizer selects the cyclic A → D → E → C → B processing sequence with profit $7791 and a cycle time of 125 h. To learn the reasons why the first production sequence turns out to be better than the second one, we need to analyze the numerical values of each one of the terms of the objective function ϕ_1, ϕ_2, and ϕ_3. Those values turn out to be [32397, 23262, 1247] and [32463, 23330, 1234] for the first and second solutions, respectively (see Table 3 for information regarding optimal values of the additional decision variables). From this information, we see that both solutions have similar ϕ_1 and ϕ_2 values. However, the difference between those solutions is the transition cost: the second solution features a larger transition cost, and this makes it suboptimal compared to the first one. Dynamic product transitions for this production sequence are depicted in Figure 5. As can be seen, the dynamic product transitions feature a shape that resembles the results of the best MIDO solution.
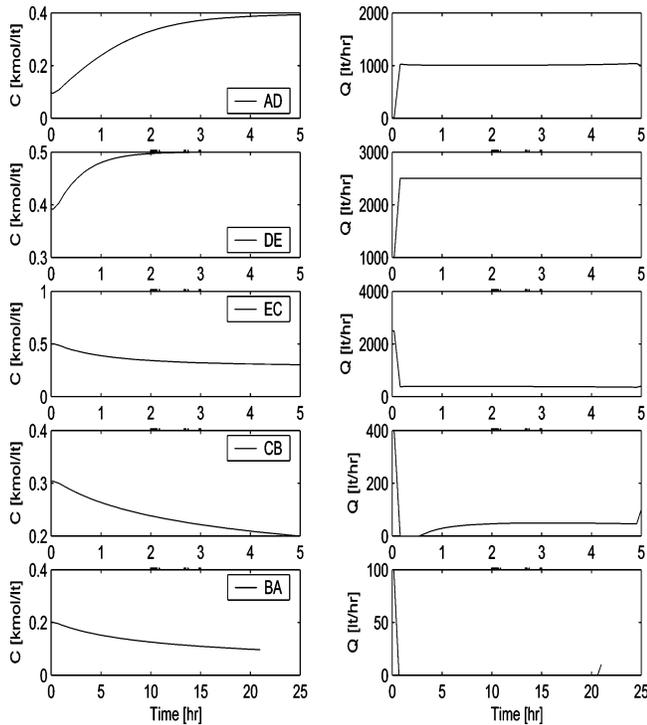
Figure 5. Optimal dynamic profiles for the volumetric flow rate and reactor concentration during product transition for the first case study, second best solution.

Figure 6. Optimal dynamic profiles for the volumetric flow rate and reactor concentration during product transition for the first case study, third best solution.

Regarding the third-best MIDO optimal solution, the optimizer selected the cyclic B → A → E → C → D production sequence with profit $6821.6 and a cycle time of 127 h. Information about the decision variables of this solution can be found in Table 4. As we can see, the third optimal solution has a larger objective function value decrease compared to the second one. Analyzing the $[\phi_1, \phi_2, \phi_3] = [31967, 23352, 1794]$ values, we notice that the third solution features a decrease in ϕ_1 (the profit

Table 4. Simultaneous Scheduling and Control Results for the First Case Study, Third Best Solution[a]

slot	product	process time (h)	production rate (kg/h)	w (kg)	transition time (h)	T start (h)	T end (h)
1	B	12.7	80	1 012.5	21	0	33.7
2	A	42.04	9.033	379.7	5	33.7	80.7
3	E	23.3	1 250	29 125.4	5	80.7	109
4	C	4.6	278.72	1 265.6	5	109	118.6
5	D	2.09	607	1 265.6	6	118.6	127

[a] The objective function value is $6821.6 and 127 h of total cycle time.

associated to product manufacture is smaller) and an increase in ϕ_3 (larger transition cost). This cost combination makes this production sequence worse than the first and second ones, even though the shape of the dynamic transitions looks similar to the first and second cases, as depicted in Figure 6. The CPU times (IBM laptop, 1.6 Ghz, Windows XP) needed for MIDO problem solution were 13.8, 67, and 27.8 s for the best, second, and third solutions, respectively.

4.2. CSTR with Simultaneous Reactions and Input Multiplicities. The following set of reactions

$$2R_1 \xrightarrow{k_1} A$$

$$R_1 + R_2 \xrightarrow{k_2} B$$

$$R_1 + R_3 \xrightarrow{k_3} C$$
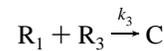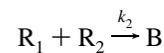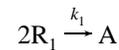
is carried out in a continuous and isothermal stirred tank reactor displayed in Figure 7. Products A, B, and C are manufactured using different values of the feed stream volumetric flow rates of the reactants R_1, R_2, and R_3.

The dynamic mathematical model of the above system is as follows.

$$\frac{dC_{R_1}}{dt} = \frac{(Q_{R_1}C_{R_1}^i - QC_{R_1})}{V} + \mathscr{R}_{r_1} \quad (26)$$

$$\frac{dC_{R_2}}{dt} = \frac{(Q_{R_2}C_{R_2}^i - QC_{R_2})}{V} + \mathscr{R}_{r_2} \quad (27)$$

$$\frac{dC_{R_3}}{dt} = \frac{(Q_{R_3}C_{R_3}^i - QC_{R_3})}{V} + \mathscr{R}_{r_3} \quad (28)$$

$$\frac{dC_A}{dt} = \frac{Q(C_A^i - C_A)}{V} + \mathscr{R}_A \quad (29)$$

$$\frac{dC_B}{dt} = \frac{Q(C_B^i - C_B)}{V} + \mathscr{R}_B \quad (30)$$

$$\frac{dC_C}{dt} = \frac{Q(C_C^i - C_C)}{V} + \mathscr{R}_C \quad (31)$$

where the kinetic expressions follow simple mass action law kinetics,

$$\mathscr{R}_A = k_1 C_{R_1}^2 \quad (32)$$

$$\mathscr{R}_B = k_2 C_{R_1} C_{R_2} \quad (33)$$

$$\mathscr{R}_C = k_3 C_{R_1} C_{R_3} \tag{34}$$

$$\mathscr{R}_{r_1} = -\mathscr{R}_A - \mathscr{R}_B - \mathscr{R}_C \tag{35}$$

$$\mathscr{R}_{r_2} = -\mathscr{R}_B \tag{36}$$

$$\mathscr{R}_{r_3} = -\mathscr{R}_C \tag{37}$$

and

$$Q = Q_{R_1} + Q_{R_2} + Q_{R_3} \tag{38}$$

where Q_{R_1}, Q_{R_2}, and Q_{R_3} are the feed stream volumetric flow rates of reactants R_1, R_2, and R_3, respectively. C^i is the reactant concentration, C is the product concentration, V is the reactor volume, and k_1, k_2, and k_3 are the kinetic rate constants. Q is the total feed stream volumetric flow rate. The design and kinetic parameters are shown in Table 5.

The operating conditions leading to the manufacture of each one of the A, B, and C products are shown in Table 6; also shown is the steady-state information concerning each product. From the information contained in this table, we see that the residence time of product A is larger than the corresponding ones of products B and C. In fact, product A features a residence time value that is exactly double products B and C residence times. This indicates that transition from any product to product A will be slower than that from product A to any other product.

In reaction systems featuring intermediate products, as the problem at hand, there is the risk of input multiplicities. This kind of nonlinear behavior creates a situation where the same state value is obtained for two different values of the manipulated variable. From a closed-loop control point, this behavior is undesirable since, under certain conditions, it has been related to the presence of right-hand plane zeros,[25] which limit the response speed of the closed-loop system. The emergence of right-hand plane zeros makes the use of proportional−integral−derivative (PID) controllers impractical because of slope sign changes.[26] Until now, the only way of dealing with input multiplicities has been to use a controller able to deal with those systems or by system redesign. In our case, for the operating and processing conditions shown in Tables 5 and 6, the reaction system displays input multiplicities as shown in Figure 8. Input multiplicities were only found for the B and C products; monotonic behavior was always observed for the A product.

Information regarding the demand rate and inventory and product costs is shown in Table 7, while simultaneous optimal scheduling and control results are shown in Table 8. As shown there, the optimizer selected the cyclic C → B → A production sequence. Figure 9 depicts the optimal state transitions for this production sequence.

Similarly to the first case of study, we found the second best optimal production sequence. The optimizer selected the cyclic A → C → B production sequence (see Figure 10). The first and second solutions feature the same objective function value, production times, process rates, etc. as shown in Table 8 for the second production sequence; the sequence in which products are manufactured is the only difference between both production sequences. The reason both production sequences feature the same values of the decision variables is due to the fact that the production sequence is cyclic and the time horizon is infinite. Hence, the sequences C → B → A and B → C → A are equivalent. Analogously to the steady-state optimal results, the dynamic optimal transition trajectories of the second and first solutions are the same. The CPU times for the MIDO problem
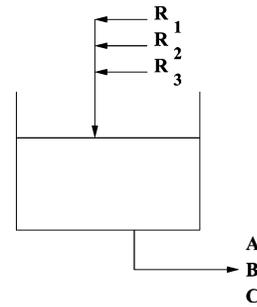
Figure 7. CSTR flowsheet for the second case study. Products (A, B, and C) are manufactured using different combinations of the reactants (R_1, R_2, and R_3).

Table 5. Steady-State Design and Kinetic Information for the Second Case Study

parameter	value	units	parameter	value	units
$C_{R_1}^i$	1	mol/L	C_C^i	0	mol/L
$C_{R_2}^i$	0.8	mol/L	V	6000	l
$C_{R_3}^i$	1	mol/L	k_1	0.1	L/(min·mol)
C_A^i	0	mol/L	k_2	0.9	L/(min·mol)
C_B^i	0	mol/L	k_3	1.5	L/(min·mol)

Table 6. Processing Conditions Leading to the Manufacture of the A, B, and C Products of the Second Case Study.[a]

prod	Q_{R_1}	Q_{R_2}	Q_{R_3}	C_{R_1}	C_{R_2}	C_{R_3}	C_A	C_B	C_C
A	100	0	0	0.333	0	0	0.666	0	0
B	100	100	0	0.1335	0.0869	0	0.0534	0.3131	0
C	100	0	100	0.0837	0	0.1048	0.021	0	0.3951

[a] The cost of the raw material (C^r) Is $5.

solution were 291 and 685 s for the best and second solutions, respectively.

4.3. CSTR with Output Multiplicities. To compute dynamic optimal transition trajectories around highly nonlinear regions, the CSTR model as proposed by Hicks and Ray[27] was used. Because the original parameters set used by these authors did not lead to multiple steady states, some of the values were modified in order to end up with a multiplicity map. In dimensionless form, the model is given by

$$\frac{dy_1}{dt} = \frac{1 - y_1}{\theta} - k_{10} e^{-N/y_2} y_1 \tag{39}$$

$$\frac{dy_2}{dt} = \frac{y_f - y_2}{\theta} + k_{10} e^{-N/y_2} y_1 - \alpha u(y_2 - y_c) \tag{40}$$

where y_1 stands for dimensionless concentration (c/c_f), y_2 is the dimensionless temperature (T/Jc_f), y_c is the dimensionless coolant temperature (T_c/Jc_f), y_f is the dimensionless feed temperature (T_f/Jc_f), and u is the cooling flowrate. Table 9 contains the numerical values of the parameters used in this work; this set of parameter values leads one to operate around the multiplicity region shown in Figure 11.

Our goal is to manufacture four products denoted as A, B, C, and D. Operating conditions are also displayed in Figure 11. Note that the A and B products are manufactured around open-loop stable steady states. The C operating point is located at the point where a stability interchange, together with a Hopf bifurcation point, takes place. Finally, the D product is manufactured around a completely unstable open-loop operating region. In all the cases, the manipulated variable is the cooling flow rate u. One of the aims of this case study is to demonstrate that, even in the face of highly nonlinear operating regions and
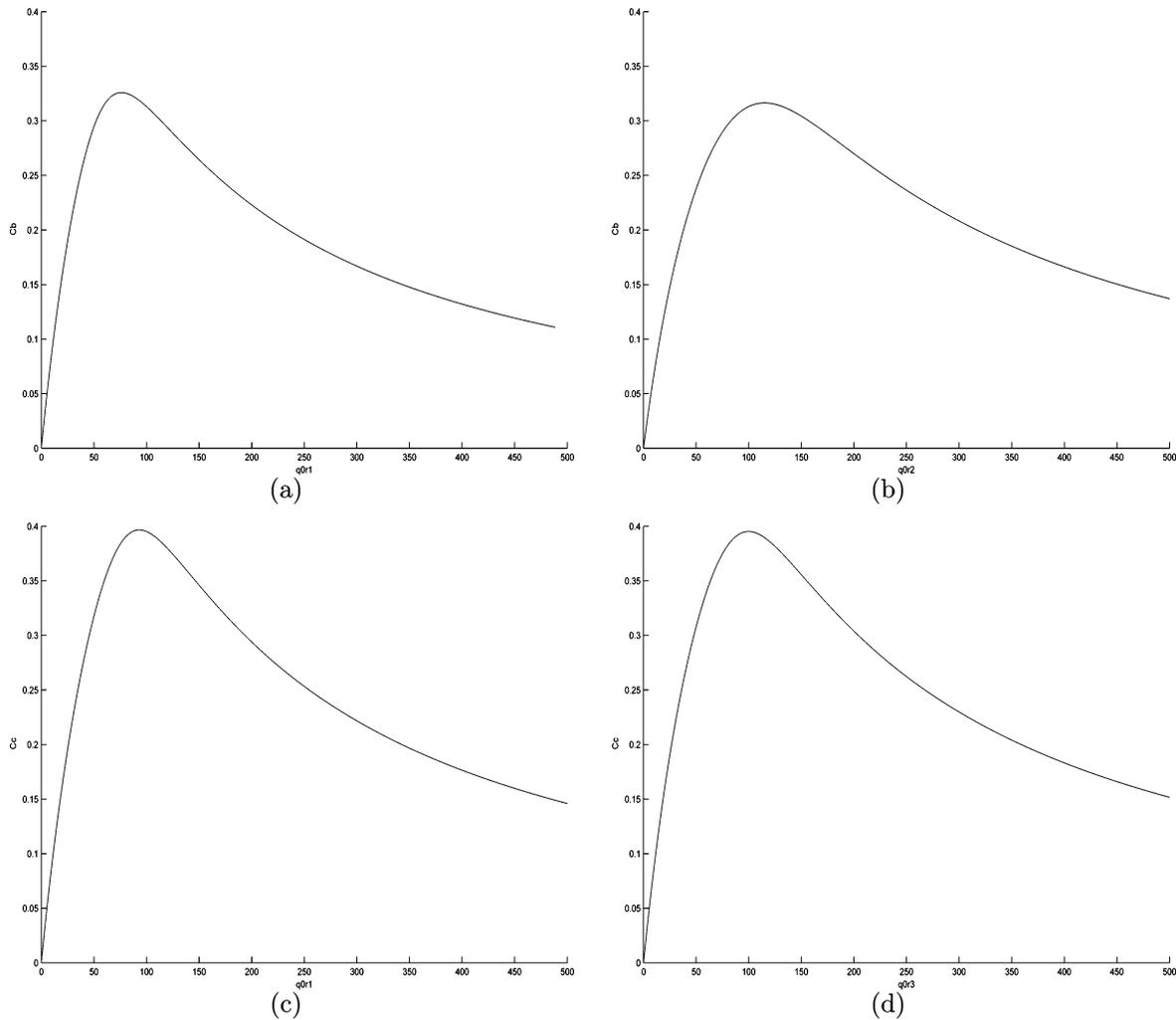
Figure 8. Input multiplicities in the second case study. (a) and (b) refer to product B using $Q_{R_1}^\circ$ and $Q_{R_2}^\circ$ as continuation parameters, respectively. Similarly, (c) and (d) refer to product C using $Q_{R_1}^\circ$ and $Q_{R_3}^\circ$ as continuation parameters, respectively, while C_b and C_c stand for composition of products B and C, respectively.

Table 7. Demand Rate and Product and Inventory Costs for the Second Case Study Reaction System

product	demand (kg/m)	product cost ($/kg)	inventory cost ($)
A	5	500	1
B	10	400	1.5
C	15	600	1.8

Table 8. Simultaneous Scheduling and Control Results for the Second Case Study[a]

slot	product	process time (m)	production rate (kg/m)	w (kg)	transition time (m)	T start (m)	T end (m)
1	C	204.2	89.52	18273.3	15	0	219.2
2	B	44.5	71.31	3174.4	15	219.2	278.7
3	A	23.8	66.7	1587.2	15	278.7	317.5

[a] The objective function value is $32 388 and 317.5 m of total cycle time.

open-loop unstable systems, our proposed simultaneous scheduling and control formulation is able to perform satisfactorily and to determine an optimal scheduling and control solution. Information regarding the production rate, demand rate, and inventory costs is shown in Table 10.

In this case, the A → B → C → D scheduling turned out to be the optimal cyclic production sequence. The profit is $7657 with a total cycle time of 100.6 h. The rest of the optimal values of the decision variables are shown in Table 11. It should be

Table 9. Parameters Values for the Third Case Study Featuring Output Nonlinearities

θ	20	residence time	T_f	300	feed temperature
J	100	$(-\Delta H)/(\rho C_p)$	k_{10}	300	preexponential factor
c_f	7.6	feed concentration	T_c	290	coolant temperature
α	1.95×10^{-4}	dimensionless heat transfer area	N	5	$E_1/(RJc_f)$

Table 10. Process Data for the Third Case Study[a]

product	demand (kg/h)	product cost ($/kg)	inventory cost ($)
A	100	100	1
B	200	50	1.3
C	400	30	1.4
D	500	80	1.1

[a] A, B, C, and D stand for the four products to be manufactured. Information about the steady-state design for each one of the products is shown in Figure 11. The cost of the raw material (C^r) Is $10.

Table 11. Simultaneous Scheduling and Control Results for the Third Case Study[a]

slot	product	process time (h)	production rate (kg/h)	w (kg)	transition time (h)	T start (h)	T end (h)
1	A	28.3	559.9	15 831.7	10	0	38.3
2	B	13.1	613.6	8 044.9	10	38.3	61.4
3	C	13.4	656.1	8 748.9	10	61.4	84.8
4	D	5.8	688.3	4 022.5	10	84.8	100.6

[a] The objective function value is $7657 and 100.6 h of total cycle time.
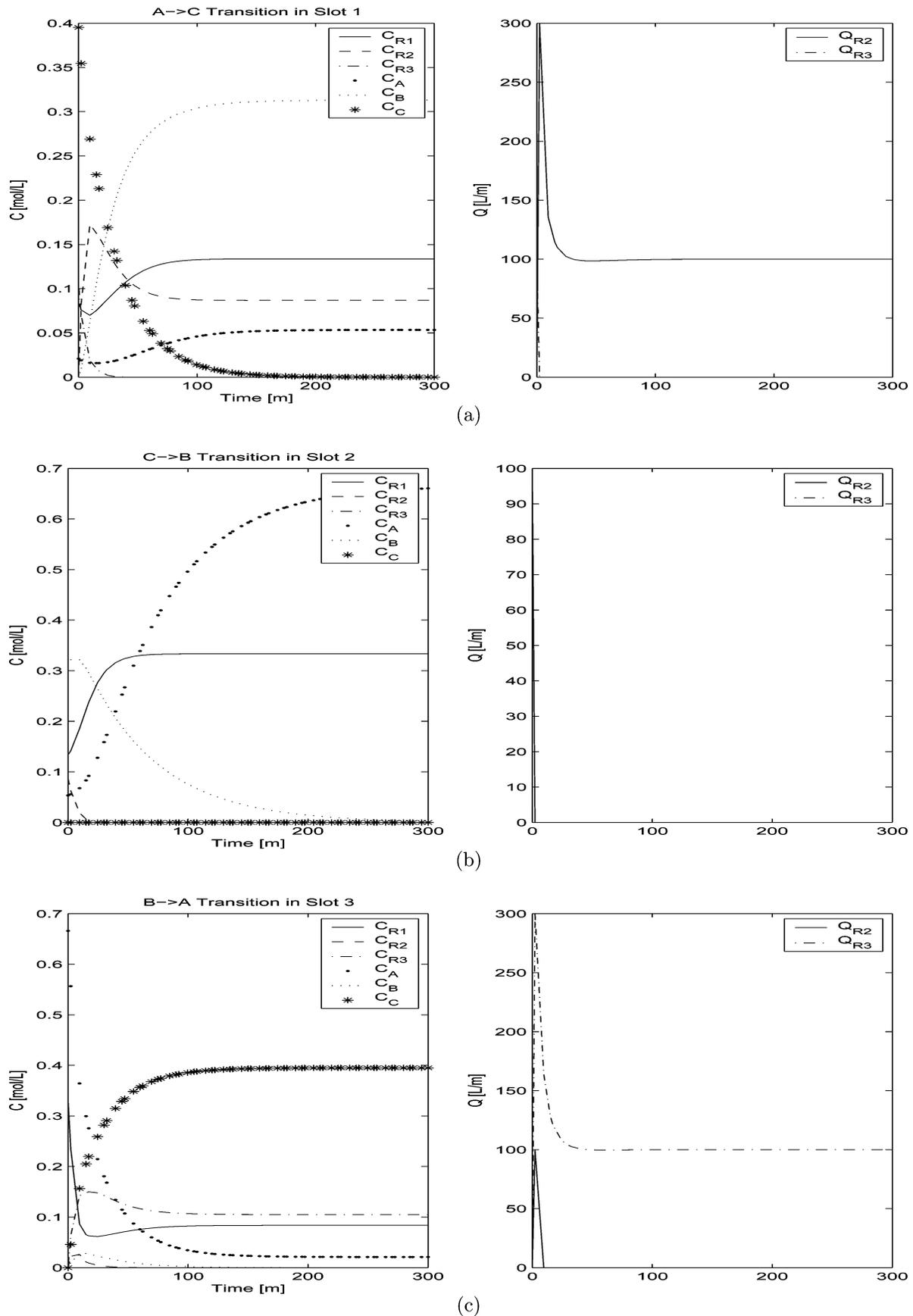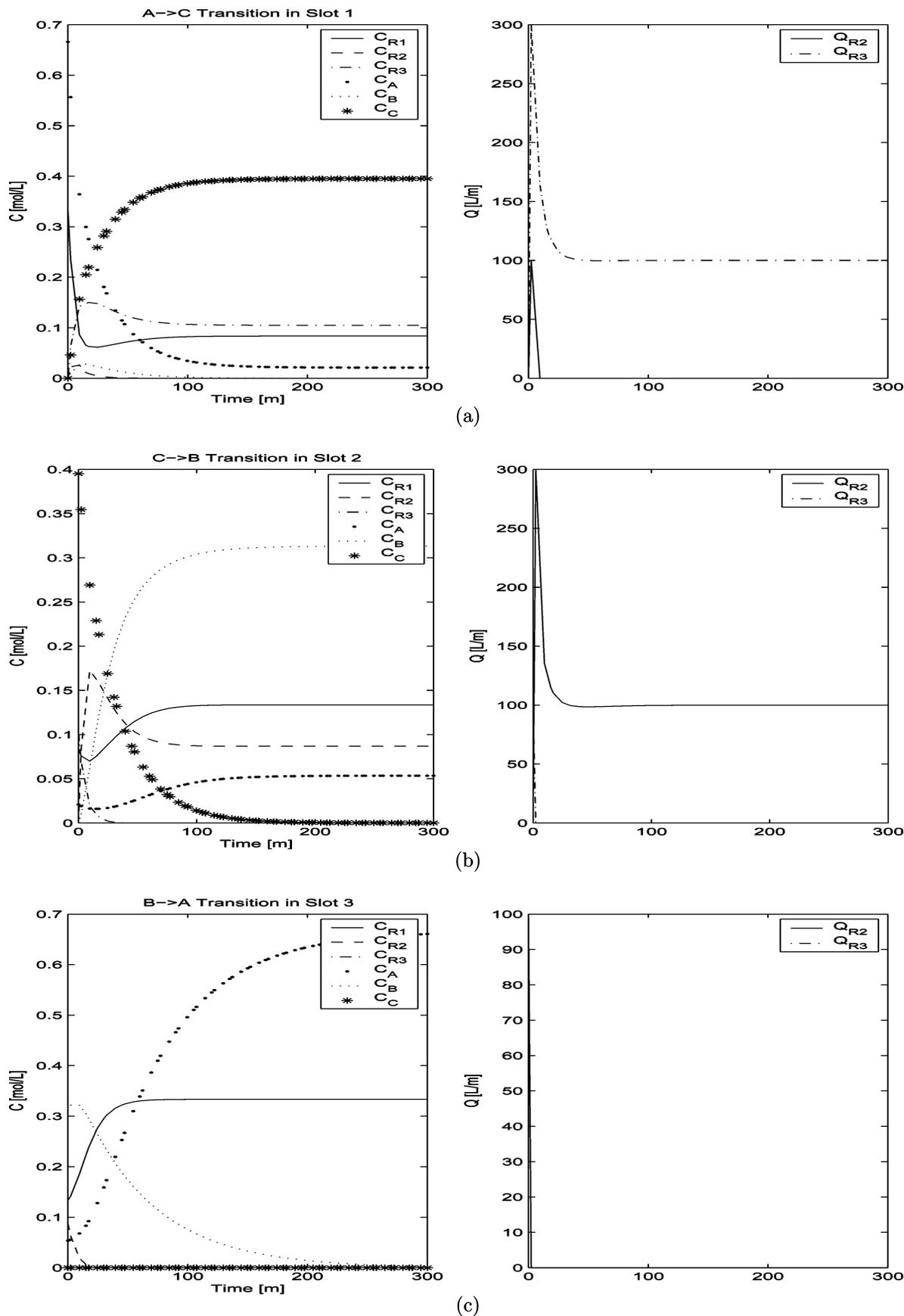
Figure 9. Optimal schedule and dynamic profiles for reactor concentrations and volumetric feed flow rates for the second example.

remarked that, in this case study, we have two products (C and D) whose manufacture demands to operate around open-loop unstable operating points. The computation of open-loop

dynamic optimal trajectories for open-loop unstable systems is difficult to carry out using dynamic optimization strategies based upon the so-called sequential approach.[28] On the other hand,

Figure 10. Optimal schedule and dynamic profiles for reactor concentrations and volumetric feed flow rates for the second example, second solution.

the simultaneous approach[29] efficiently and naturally deals with this type of problem without using tricks such as closed-loop stabilization of the originally unstable system and then running the dynamic optimization problem. In a previous work,[29] we have provided some theoretical explanations why the simultaneous approach copes with open-loop unstable systems. Not

Table 12. Open-Loop Poles for Products A, B, C, and D of the Third Case Study

	product			
pole	A	B	C	D
1	$-0.1352 + 0.1566i$	$-0.0430 + 0.1548i$	$0.0164 + 0.1147i$	$0.0524 + 0.0440i$
2	$-0.1352 - 0.1566i$	$-0.0430 - 0.1548i$	$0.0164 - 0.1147i$	$0.0524 - 0.0440i$

Table 13. Simultaneous Scheduling and Control Results for the Third Case Study, Second Solution[a]

| slot	product	process time (h)	production rate (kg/h)	w (kg)	transition time (h)	T start (h)	T end (h)
1	D	6.07	559.9	4176.7	10	0	16.07
2	A	28.9	613.6	16177.2	10	16.07	55
3	C	13.9	656.1	9084.3	12	55	80.8
4	B	13.7	688.3	8353.4	10	80.8	104.4

[a] The objective function value is $6070.6 and 104.4 h of total cycle time.
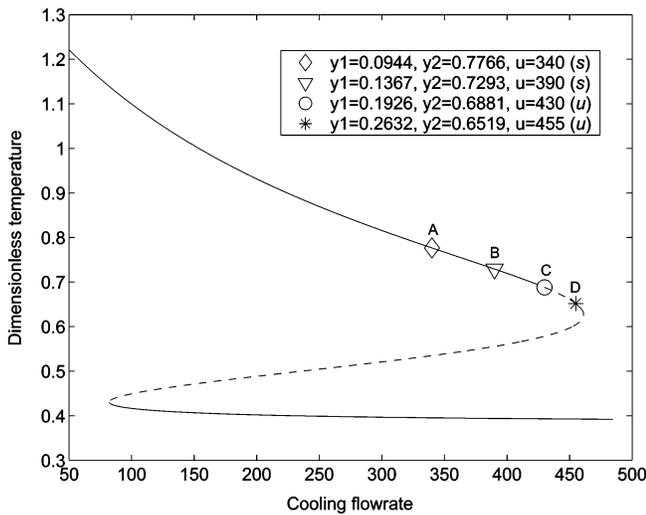
Figure 11. Multiplicity map (— stable solution, − − unstable solution).
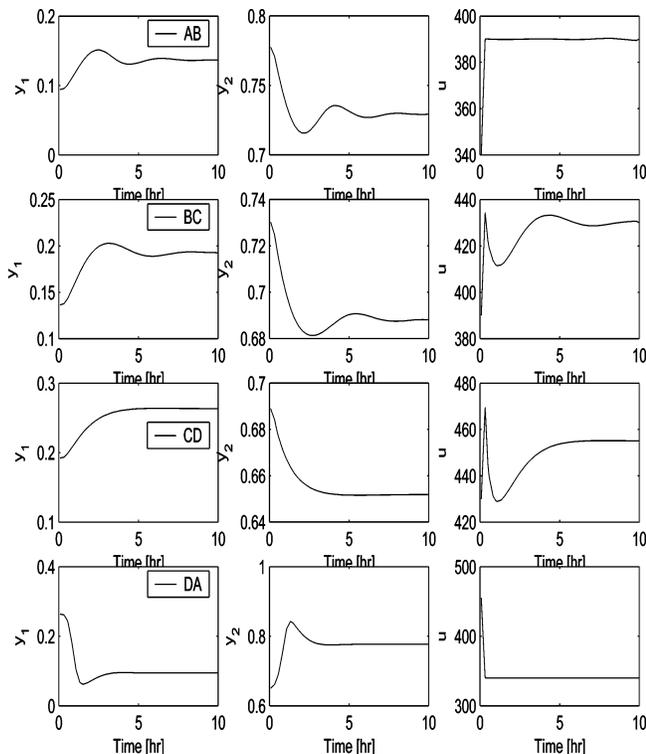
Figure 12. Optimal schedule and dynamic profiles for the third case study.

surprisingly, the minimum transition time, independently of the type of transition, is 10 h. This result is in agreement with previous calculations related to the open-loop dynamic optimization of the same reaction system.[30] Another point to stress is that our SSC formulation is able to cope with product transitions between highly nonlinear regions. As a matter of fact, the B → C transitions involves transition from an open-loop stable to an unstable system through a Hopf bifurcation point where oscillatory behavior emerges.

From the open-loop poles shown in Table 12, we should expect to have an oscillatory response for product transitions because most of the poles have a nonzero imaginary part. Product transitions ending at product D should feature the weakest oscillatory behavior because its imaginary part is rather small. These observations are supported by looking at the dynamic profiles of both the manipulated and controlled variables as depicted in Figure 12. Moreover, we would like to highlight the fact that the nonlinear nature of the product transitions addressed in this case study can also be appreciated in the dynamic behavior of the manipulated variable u. In the previous two case studies, the manipulated variable(s) always featured a simple steplike form mainly due to the presence of mild nonlinearities embedded into the system. However, in the present case study, the dynamic optimal shape of the manipulated variable is not obvious. This is particularly true for the B → C and the C → D product transitions that are placed deeper into the unstable region.

For comparison purposes of the present solution, we found a second suboptimal solution featuring the cyclic D → A → C → B production sequence. In this case, the objective function value was $6070.6 and 104.4 of total cyclic time. The rest of the optimal values of the decision variables are shown in Table 13. This solution is suboptimal because the optimizer decided first to manufacture product D and from there to carry out the product transition for starting the manufacture of product A. This product transition turns out to be more expensive because it is hard to perform, since it involves the widest variation in the open-loop pole location. From there, the optimizer keeps making product transitions that are not the best ones in terms of the transition costs. From product A, the optimizer selects to carry out a transition toward product C and from here to product B. Those product transitions are definitely not the best ones in terms of transition costs. To support the past statements, we computed the ϕ_1, ϕ_2, and ϕ_3 terms, as defined in eqs 2−4, of the objective function of the present case study. For the first optimal solution, these values turn out to be [ϕ_1, ϕ_2, ϕ_3] = [25553.2, 17633.8, 263], while for the second suboptimal solution those values are [25303, 18252, 981], in the same order. From this comparison, we can see that the profit associated with product manufacture and inventory costs are similar for both production sequences. The main difference lies in the transition costs. This explains why the cyclic D → A → C → B production sequence is a suboptimal solution. The dynamic profiles of both system states and the manipulated variable are depicted in Figure 13. Again, the nonlinear behavior embedded into the present system can be seen in the shape of the manipulated variable between product transitions. The CPU times for MIDO problem solution were 254 and 47 s for the best and second solutions, respectively.
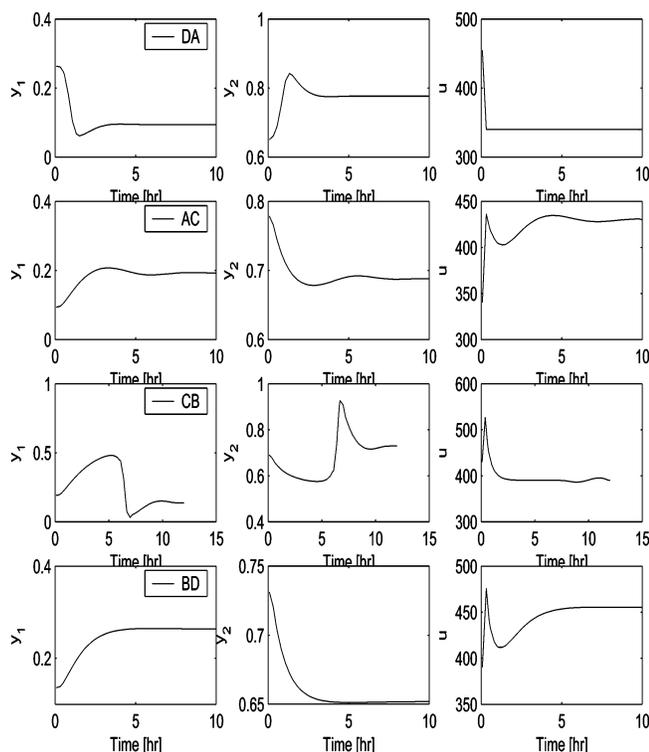
Figure 13. Optimal schedule and dynamic profiles for the third case study, second best solution.

5. Conclusions

In this work, we have addressed the simultaneous cyclic scheduling and control problem for several multiproduct CSTRs. Rather than assuming constant transition times and neglecting process dynamics, a mathematical model, able to describe dynamic process behavior during product transition, was embedded into the optimization formulation. Solving the scheduling and control problem taking into account process dynamics is the rigorous way to address scheduling problems.

Because highly optimized chemical processes tend to operate around nonlinear operating regions, we selected as case studies three problems involving reaction systems, two of which display highly nonlinear behavior in the form of input and output multiplicities, Hopf bifurcation points, and open-loop unstable operating regions. Even in the face of nonlinear behavior, the proposed simultaneous cyclic scheduling and control formulation was able to find optimal production sequences. However, convergence toward the optimal solution turned out to be harder to achieve as the nonlinearity of the system increased. Moreover, the presence of nonlinearities creates nonconvexities in the optimization formulation, probably leading to suboptimal solutions.

From the results of the third example, we notice that the performance of SBB for finding MIDO optimal solutions was superior to the one displayed by DICOPT. It is well-known that the strength of DICOPT lies in solving problems with large number of binary variables and mild nonlinearities. On the other hand, SBB should produce better results for systems with a relatively small number of binary variables but harder nonlinearities. This was indeed the behavior observed from both solvers in example 3, which is the one that mainly features these characteristics.

It should be noticed that the scheduling and control problem is addressed in an open-loop manner (e.g., no control system is present). In this approach, once the sequence order and optimal control policies are determined, one should then decide how to closed-loop track such optimal trajectories.[31] In fact, this is one of the major advantages of the simultaneous dynamic optimization approach over other dynamic optimization approaches (e.g., sequential approaches). Our approach is able to deal with state transitions, even if the initial or final (or both) steady states are open-loop unstable.[29] If the sequential approach for optimal transition involving open-loop unstable steady states is used, such a procedure will not succeed in computing such trajectories, simply because, since sequential approaches use numerical integration for optimal trajectories computation, it is well-known that unstable steady states cannot be reached by numerical integration. Therefore, before computing optimal transition trajectories, the sequential approach requires that all the unstable modes be removed. Most of the time, this is done by incorporating a feedback controller. However, in this case, the optimal transition will depend on the sort of controller and the way in which it was tuned.

In this work, only local solutions to the resulting discretized MINLPs were sought. Presently, the computation of global solutions to NLP problems does not seem to be an easy task. The available software (e.g., BARON[32]) tends to work efficiently mostly for small- and medium-size problems with mild nonlinearities. The complexity problem grows when dealing with MINLPs. Because of these reasons and to keep computational complexity on a reasonable level, in this work we only used local MINLPs solution techniques such as that embedded in the DICOPT solver. Of course, the computation of global MIDO solutions is a problem that deserves to be seriously considered, and we hope to address this problem in the future.

It must be stressed that, for solving the resulting MIDO problems, no special initialization method was used. Only initial estimates for the states and manipulated variables were provided. To obtain such initial estimates, linear interpolations between the initial and final states and manipulated variables were used. Using the DICOPT and SBB programs, no initialization of the integer variables is needed, since the programs obtained them by initially solving a relaxed NLP problem. Of course, valid lower and upper bounds on all the continuous decision variables have to be imposed, but most of the time they are easy to propose. The GAMS files used for solving the examples discussed in this paper are available to interested readers to make sure they can indeed reproduce our results.

From the results obtained in this work, dealing with larger-dimension systems featuring stronger nonlinear behavior, MIDO formulations, like the one presented, need to be improved to cope with complex dynamic systems. The direct solution of MIDO problems for systems with the above-mentioned characteristics does not look feasible, and it might require excessive CPU time. Therefore, a decomposition strategy that exploits the natural structure of scheduling and control MIDO problems needs to be developed. Other interesting extensions of the present work consist of the case when several reactors operate in parallel[33] and of the simultaneous optimization of planning, scheduling, and control.[34,35]

Nomenclature

Indices

products = i, p = 1, ..., N_p
slots = k = 1, ..., N_s
finite elements = f = 1, ..., N_{fe}

collocation points $= c$, $l = 1, ..., N_{cp}$
system states $= n = 1, ..., N_x$
manipulated variables $= m = 1, ..., N_u$

Decision Variables

y_{ik} = binary variable to denote if product i is assigned to slot k
y'_{ik} = binary auxiliary variable
z_{ipk} = binary variable to denote if product i is followed by product p in slot k
p_k = processing time at slot k
t_k^e = final time at slot k
t_k^s = start time at slot k
t_{fck} = time value inside each finite element k and for each internal collocation point c
G_i = production rate
T_c = total production wheel time (h)
x_{fck}^n = nth system state in finite element f and collocation point c of slot k
u_{fck}^m = mth manipulated variable in finite element f and collocation point c of slot k
W_i = amount produced of each product (kg)
θ_{ik} = processing time of product i in slot k
θ_k^t = transition time at slot k
Θ_i = total processing time of product i
$x_{o,fk}^n$ = nth state value at the beginning of the finite element f of slot k
$\bar{x}_k^n$ = desired value of the nth state at the end of slot k
$\bar{u}_k^m$ = desired value of the mth manipulated variable at the end of slot k
$x_{in,k}^n$ = nth state value at the beginning of slot k
$u_{in,k}^n$ = mth manipulated variable value at the beginning of slot k
X_i = conversion

Parameters

N_p = number of products
N_s = number of slots
N_{fe} = number of finite elements
N_{cp} = number of collocation points
N_x = number of system states
N_u = number of manipulated variables
D_i = demand rate (kg/h)
C_i^p = price of products ($/kg)
C_i^s = cost of inventory [$/(kg/h)]
C^r = cost of raw material ($)
h_{fk} = length of finite element f in slot k
$\Omega_{N_{cp}, N_{cp}}$ = matrix of Radau quadrature weights
θ^{max} = upper bound on processing time
t_{ip}^t = estimated value of the transition time between product i and p
$x_{ss,i}^n$ = nth state steady value of product i
$u_{ss,i}^m$ = mth manipulated variable value of product i
F^o = feed stream volumetric flow rate
X_i = conversion degree
x_{min}^n, x_{max}^n = minimum and maximum value of the state x^n
u_{min}^m, u_{max}^m = minimum and maximum value of the manipulated variable u^m
$\gamma_{N_{cp}}$ = roots of the Lagrange orthogonal polynomial

Literature Cited

(1) Mendéz, C. A.; Cerda, J.; Grossmann, I. E.; Harjunkoski, I.; Fahl, M. State of the Art Review of Optimization Methods for Short-Term Scheduling of Batch Processes. **2005**, submitted for publication.

(2) Biegler, L. T. Optimization strategies for complex process models. *Adv. Chem. Eng.* **1992**, *18*, 197−256.

(3) Feather, D.; Harrell, D.; Lieberman, R.; Doyle, F. J. Hybrid Approach to Polymer Grade Transition Control. *AIChE J.* **2004**, *50* (10), 2502−2513.

(4) Bhatia, T.; Biegler, L. T. Dynamic Optimization in the Design and Scheduling of Multiproduct Batch Plants. *Ind. Eng. Chem. Res.* **1996**, *35*, 2234−2246.

(5) Mahadevan, R.; Doyle, F. J.; Allcock, A. C. Control-Relevant Scheduling of Polymer Grade Transitions. *AIChE J.* **2002**, *48* (8), 1754−1764.

(6) Mishra, B. V.; Mayer, E.; Raisch, J.; Kienle, A. Short-Term Scheduling of Batch Processes. A Comparative Study of Differentes Approaches. *Ind. Eng. Chem. Res.* **2005**, *44*, 4022−4034.

(7) Nystrom, R. H.; Franke, R.; Harjunkoski, I.; Kroll, A. Production Campaing Planning Including Grade Transition Sequencing and Dynamic Optimization. *Comput. Chem. Eng.* **2005**, *29* (10), 2163−2179.

(8) Birewar, D.; Grossmann, I. E. Incorporating scheduling in the optimal design of multiproduct batch plants. *Comput. Chem. Eng.* **1989**, *13*, 141.

(9) Chatzidoukas, C.; Kiparissides, C.; Perkins, J. D.; Pistikopoulos, E. N. Optimal Grade Transition Campaign Scheduling in a Gas-Phase Polyolefin FBR Using Mixed Integer Dynamic Optimization. In *Process System Engineering*; Elsevier: New York, 2003; pp 744−747.

(10) Allgor, R. J.; Barton, P. Mixed-Integer Dynamic Optimization I: Problem Formulation. *Comput. Chem. Eng.* **1999**, *23* (4−5), 567−584.

(11) Smania, P.; Pinto, J. M. Mixed Integer Nonlinear Programming Techniques for the Short Term Scheduling of Oil Refineries. In *Process System Engineering*; Elsevier: New York, 2003; pp 744−747.

(12) Biegler, L. T. *An overview of simultaneous strategies for dynamic optimization*; Manuscript in revision, 2006.

(13) Kameswaran, S.; Biegler, L. T. Simultaneous Dynamic Optimization Strategies: Recent Advances and Challenges. In *Proceedings of CPC 7*; 2006, accepted for publication.

(14) Avraam, M.; Shah, N.; Pantelides, C. Modeling and optimization of general hybrid systems in continuous plant domain. *Comput. Chem. Eng.* **1998**, *22*, S221−S228.

(15) Mohideen, M. J.; Perkins, J. D.; Pistikopoulos, E. N. Towards an efficient numerical procedure for mixed integer optimal control. *Comput. Chem. Eng.* **1997**, *21*, S457−S462.

(16) Bansal, V.; Sakizlis, V.; Ross, R.; Perkins, J. D.; Pistikopoulos, E. N. Towards an efficient numerical procedure for mixed integer optimal control. *Comput. Chem. Eng.* **1997**, *21*, S457−S462.

(17) Chachuat, B.; Singer, A. B.; Barton, P. I. Global Mixed-Integer Dynamic Optimization. *AIChE J.* **2005**, *51* (8), 2235−2253.

(18) Flores-Tlacuahuac, A.; Biegler, L. T. A Robust and Efficient Mixed-Integer Non-Linear Dynamic Optimizaion Approach for Simultaneous Design and Control. In *European Symposium on Computer Aided Process Engineering-15*; Puigjaner, L., Espuna, A., Eds.; Elsevier: New York, 2005; pp 67−72.

(19) Duran, M. A.; Grossmann, I. E. An outer approximation algorithm for a class of mixed integer nonlinear programs. *Math. Prog.* **1986**, *36*, 307.

(20) Viswanathan, J.; Grossmann, I. E. A Combined Penalty Function and Outer-Approximation Method for MINLP Optimization. *Comput. Chem. Eng.* **1990**, *14* (7), 769−782.

(21) Pinto, J. M.; Grossmann, I. E. Optimal Cyclic Scheduling of Multistage Continuous Multiproduct Plants. *Comput. Chem. Eng.* **1994**, *18* (9), 797−816.

(22) Finlayson, B. *Nonlinear Analysis in Chemical Engineering*; McGraw-Hill: New York, 1980.

(23) Villadsen, J.; Michelsen, M. *Solution of Differential Equations Models by Polynomial Approximation*; Prentice-Hall: New York, 1978.

(24) Seider, W.; Brengel, D.; Provost, A.; Widagdo, S. Nonlinear Analysis in Process Design. Why Overdesign To Avoid Complex Nonlinearities? *Ind. Eng. Chem. Res.* **1990**, *29*, 805.

(25) Sistu, P.; Bequette, B. W. Model Predictive Control of Process with Input Multiplicities. *Chem. Eng. Sci.* **1995**, *50* (6), 921−936.

(26) Koppel, L. B. Input Multiplicities in Nonlinear Multivariable Control Systems. *AIChE J.* **1982**, *28* (6), 935−945.

(27) Hicks, G. A.; Ray, W. H. Approximation Methods for Optimal Control Synthesis. *Can. J. Chem. Eng.* **1971**, *40*, 522−529.

(28) Vassiliadis, V. S.; Sargent, R. W. H.; Pantelides, C. C. Solution of a class of multistage dynamic optimization problems. 1. Problems without path constraints. *Ind. Eng. Chem. Res.* **1994**, *33* (9), 2111−2122.

(29) Flores-Tlacuahuac, A.; Biegler, L. T.; Saldívar-Guerra, E. Dynamic optimization of hips open-loop unstable polymerization reactors. *Ind. Eng. Chem. Res.* **2005**, *44* (8), 2659−2674.

(30) Silva-Beard, A.; Flores-Tlacuahuac, A.; Arrieta-Camacho, J. C. *European Symposium on Computer Aided Process Engineering—12*; Elsevier: New York, 2002; pp 547−552.

(31) Flores-Tlacuahuac, A.; Alvarez, J.; Saldívar-Guerra, E.; Oaxaca, G. Process and control designs of robust transitions for exothermic continuous reactors. *AIChE J.* **2005**, *51* (3), 895−908.

(32) Tawarmalani, M.; Sahinidis, N. V. *Convexification and Global Optimization in Continuous and Mixed-Integer Nonlinear Programming: Theory, Algorithms, Software, and Applications*; Kluwer Academic Publishers: Norwell, MA, 2002.

(33) Sahinidis, N.; Grossmann, I. E. MINLP Model for Cyclic Multiproduct Scheduling on Continuous Parallel Lines. *Comput. Chem. Eng.* **1991**, *15* (2), 85−103.

(34) Grossmann, I. E. Enterprise-wide Optimization: A New Frontier in Process Systems Engineering. *AIChE J.* **2005**, *51* (7), 1846−1857.

(35) Erdirik Dogan, M.; Grossmann, I. E. A Decomposition Method for the Simultaneous Planning and Scheduling of Single Stage Continuous Multiproduct Plants. *Ind. Eng. Chem. Res.* **2006**, *45*, 299−315.